SELF-CONSISTENT CALCULATIONS OF FINITE TEMPERATURE NUCLEAR RESPONSE FUNCTION

H. SAGAWA and G.F. BERTSCH
National Superconducting Cyclotron Laboratory, Michigan State University, East Lansing, MI 48824-1321, USA

Received 23 May 1984
Revised manuscript received 9 July 1984

The nuclear response function of ^{40}Ca is studied at finite temperature using self-consistent RPA. We find that the isovector dipole strength function is quite independent of temperature up to $T \sim 6$ MeV. In contrast, the quadrupole strength function is much affected, showing a softening of the nucleus with increased temperature.

Finite temperature nuclear dynamics has recently been the subject of much study [1–5], stimulated by the finding of giant dipole resonances built on states above the yrast line [6–8]. These observations give new information about the shape and dynamics of hot nuclei. The temperature dependence of collective excitations also bears on the deep inelastic scattering process in heavy ion collisions.

So far, theoretical studies of collective excitations in hot nuclei have been done using the random phase approximation (RPA) with schematic interactions and wave functions based on the harmonic oscillator or Woods–Saxon potential [1–5]. It is of interest to go beyond these simple models to self-consistent Hartree–Fock and RPA theory, which has been shown to be well-founded and very successful in describing various kinds of collective excitations at zero temperature. Moreover, the RPA response function can be solved in coordinate space avoiding truncation of the particle–hole (p–h) configuration space and gives a proper account of the particle continuum effect.

In this paper, we study the response function at finite temperature in self-consistent RPA. We apply the Green's function method in coordinate space developed by Bertsch and Tsai [9]. The finite temperature theory is derived from the grand canonical partition function D of the system [1,2]. The expectation value for any observable of the system is given by averaging over the partition function. In this way, the density $\rho(T)$ at temperature T is given by

$$\rho(T) = \mathrm{Tr}\{D\hat{\rho}(\boldsymbol{r})\} = \sum_i f_i(T)(2j_i+1)\,\phi_i^*(\boldsymbol{r})\,\phi_i(\boldsymbol{r}), \quad (1)$$

where $\phi_i(\boldsymbol{r})$ is the single-particle wave function and $f_i(T)$ is the occupation probability of the single-particle state,

$$f_i(T) = 1/\{1 + \exp[(\epsilon_i - \epsilon_\mathrm{F})/T]\}\,. \quad (2)$$

The chemical potential ϵ_F is determined by subsidiary conditions of proton and neutron number conservation. The thermal excitation energy E^* of the equilibrated system in the independent quasiparticle approximation is given by

$$E^*(T) = \sum_i (2j_i+1) \times [f_i(T)\,\epsilon_i(T) - f_i(T=0)\,\epsilon_i(T=0)]\,. \quad (3)$$

To study the response of the system, we add a time-dependent external field $F(\boldsymbol{r})$ to the Hartree–Fock hamiltonian,

$$H(T,t) = H(T) + F(\boldsymbol{r})\exp(-\mathrm{i}\omega t) + F^*(\boldsymbol{r})\exp(\mathrm{i}\omega t)\,. \quad (4)$$

This will induce a perturbation term in the density,

$$\rho(T,t) = \rho_0(T) + [\delta\rho(T)\exp(-\mathrm{i}\omega t) + \mathrm{h.c.}]\,. \quad (5)$$

The linearized time-dependent Hartree–Fock hamiltonian is now given by

0370-2693/84/$03.00

$$H(T, t) = H_0(T) + [\delta\rho(\delta U/\delta\rho)\exp(-i\omega t) + F(r)\exp(-i\omega t) + \text{h.c.}] , \quad (4')$$

where $H_0(T) = K + U$ is the Hartree–Fock hamiltonian at finite temperature. We assume that the Hartree–Fock potential U is a function of the local density $\rho_0(T)$ which is the case for the Skyrme-type hamiltonian. The TDHF equation

$$[H(T, t) - \epsilon_i(T)]\ \phi_i(T, t) = i\partial\phi_i(T, t)/\partial t \quad (6)$$

can then be solved for the density oscillation $\delta\rho$ by the Green's function

$$\delta\rho(r, T) = G_{\mathrm{RPA}} \cdot F , \quad (7)$$

where G_{RPA} is obtained by solving the RPA equation,

$$G_{\mathrm{RPA}}(\omega, T) = G^{(0)}(\omega, T) + G^{(0)}(\omega, T)(\delta U/\delta\rho)\, G_{\mathrm{RPA}} . \quad (8)$$

In eq. (8), $G^{(0)}$ is the bare particle–hole Green's function defined by

$$G^{(0)}(r, r'; \omega, T) = \sum_{\mathrm{p,h}} f_{\mathrm{h}}(T)\, \phi^*_{\mathrm{h}}(r)[1 - f_{\mathrm{p}}(T)]\, \phi_{\mathrm{p}}(r) \times [(\omega + i\eta - \epsilon_{\mathrm{p}} + \epsilon_{\mathrm{h}})^{-1} - (\omega + i\eta + \epsilon_{\mathrm{p}} - \epsilon_{\mathrm{h}})^{-1}] \times \phi^*_{\mathrm{p}}(r')\, \phi_{\mathrm{h}}(r') . \quad (9)$$

The $f_{\mathrm{p}}(T)$ terms in eq. (9) drop out by cancellation of the forward and backward amplitude. The strength distribution of the RPA response is now obtained by the imaginary part of the Green's function,

$$S(\omega, T) = \pi^{-1}\mathrm{Tr}\{F^*\ \mathrm{Im}[G_{\mathrm{RPA}}(\omega, T)]\ F\} \quad (10)$$

for the one-body operator $F(r)$. In this derivation, we have assumed that the external field has a frequency large compared to the collision rate between quasi-particles.

The main features of the strength function are conveniently discussed in terms of sum rules. We define a kth energy moment of the excitation operator in the ensemble by

$$m_k(T) = \int_{-\infty}^{\infty} S_T(\omega)\, \omega^k\, d\omega . \quad (11)$$

where S_T is the strength function given by

$$S_T(\omega) = \frac{1}{Z}\sum_{n,m} \exp[-(E_m - \epsilon_{\mathrm{F}}N_m)/T] \times |\langle n|F|m\rangle|^2\, \delta(\omega - (E_n - E_m)) .$$

The value Z represents the partition function of the system and N_n and E_n are the number of particles and the energy of the state n. For $k = 1$, the sum (EWSR) may be evaluated in an analytic form similar to the zero temperature sum rule [2]. For multipolarity λ, this needs

$$m_1(T) = \tfrac{1}{2}\langle [F^*, [H, F]]\rangle = \frac{\hbar^2}{2m}\frac{Z^2}{A}\frac{\lambda(2\lambda+1)^2}{4\pi}\langle r^{2\lambda-2}\rangle_T \quad \text{for IS} , = \frac{\hbar^2}{2m}\frac{NZ}{A}\frac{\lambda(2\lambda+1)^2}{4\pi}\langle r^{2\lambda-2}\rangle_T(1+\kappa) \quad \text{for IV} , \quad (12)$$

where the mean square radius and the enhancement factor are defined as

$$\langle r^{2\lambda-2}\rangle_T = \int \rho_0(T)\, r^{2\lambda-2}\, dr/A ,$$

$$\kappa = (2m/\hbar^2)[t_1(1 + \tfrac{1}{2}x_1) + t_2(1 + \tfrac{1}{2}x_2)] \times \frac{1}{A}\int \rho_0^2(r)\, dr . \quad (13)$$

In eq. (13), t_1, t_2, x_1, x_2 are the usual Skyrme parameters defined in ref. [10]. The RPA sum rules are calculated from the RPA response as

$$m_k(T) = \int_0^{\infty} d\omega\, \pi^{-1}\langle F^*\ \mathrm{Im}[G_{\mathrm{RPA}}]\ F\rangle\, \omega^k . \quad (11')$$

The sum rule is exactly satisfied for $k = 1$, as shown by Vautherin and Vinh Mau [5].

We calculated the isoscalar (IS) quadrupole and isovector (IV) dipole excitations in ^{40}Ca at several temperatures. We use the Skyrme interaction SGII for the H–F and RPA calculations [11]. The parameter set SGII has been successful for the description of collective p–h excitations, while reproducing empirical ground-state properties quite well. The space of hole states is taken to include all bound single particle states up to and including the f–p shell. The space for

Table 1
RPA results for IS quadrupole states (E2) in ^{40}Ca as a function of temperature T. The thermal excitation energy E^* and the mean square radius are defined in eqs. (3) and (13), respectively. The sum rule value m_1(a) is calculated from the analytic expression (12), while the result m_1(b) is obtained by the RPA response shown in fig. 1. The non-energy-weighted and inverse-energy-weighted sum rules m_0 and m_{-1} are also obtained by the RPA results.

T (MeV)	E^* (MeV)	$\langle r^2\rangle_T$ (fm^2)	m_1(fm^4 MeV) case (a)	m_1(fm^4 MeV) case (b)	m_0 (fm^4)	m_{-1} (fm^4 MeV^{-1})	$E_1 = (m_1/m_{-1})^{1/2}$	m_0 (E_X<10 MeV)
0.0	0	11.26	9.28×10^3	8.99×10^3	526.1	31.11	17.00	0.0
1.5	10.49	11.39	9.39×10^3	9.42×10^3	593.9	47.09	14.14	61.0
3.0	37.67	11.74	9.68×10^3	9.50×10^3	676.8	74.37	11.30	167.5
6.0	99.54	12.47	1.03×10^4	9.93×10^3	714.0	107.4	9.62	167.9

the particle states includes the discrete states as well as the unbound continuum, which we treat exactly using the single-particle Green's function. The H–F wave functions and energies are taken to be T-independent since H–F properties have only a small T-dependence [5]. Since our effective interaction has a density dependent term, the p–h interaction shows T-dependence through the equilibrium density $\rho_0(T)$.

The results of isoscalar E2 excitations are shown in table 1 and fig. 1. The RPA result at T = 0 MeV gives a collective resonance at E_X = 16.7 MeV with the width at half-maximum Γ = 400 keV exhausting 70% of EWSR. Empirical evidence has been reported at around E_X = 17 MeV having $\frac{2}{3}$ of the EWSR value [12]. There is no transition strength below E_X = 10 MeV in the result at T = 0 MeV. However, at finite temperature, the Fermi surface is melted and the $0\hbar\omega$ p–p and h–h excitations become possible together with the $2\hbar\omega$ p–h excitation which is only allowed in the T = 0 MeV case. The p–p and h–h configurations change mainly the strength distribution at the low-energy side at E_X = 4 MeV. The sum of the strength below E_X = 10 MeV is going up to 20% of the total strength at the temperature T = 3 MeV. On the con-

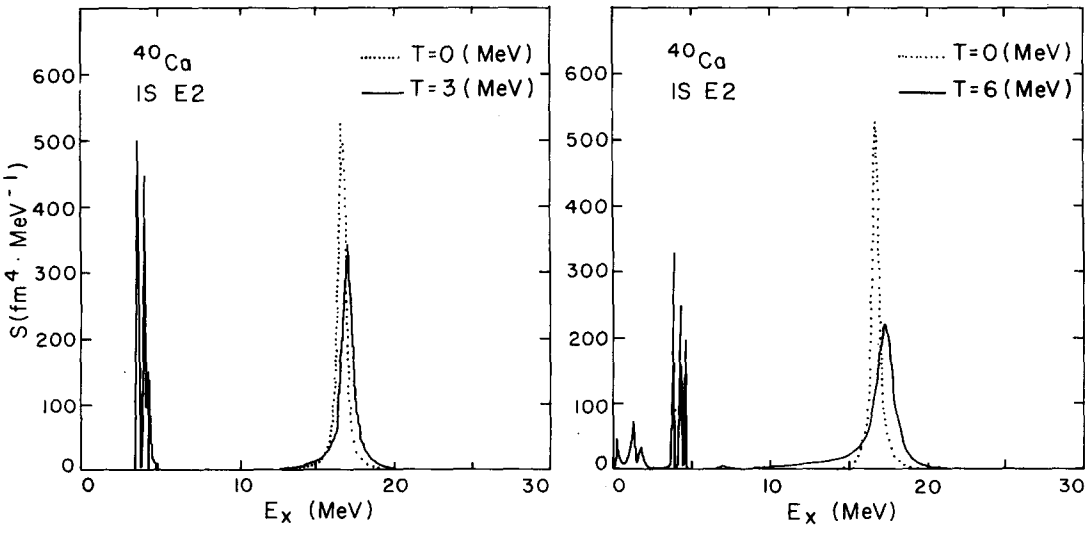

Fig. 1. RPA strength distributions of the IS quadrupole operator $F(r) = \frac{1}{2}\Sigma_i(1 - \langle\tau_{zi}\rangle)\, r_i^2\, Y_{2m}(\hat{r}_i)$ in ^{40}Ca at finite temperatures. The dotted curve shows the result of T = 0 MeV, while the solid curves at LHS and RHS show the results of T = 3 MeV and T = 6 MeV, respectively.

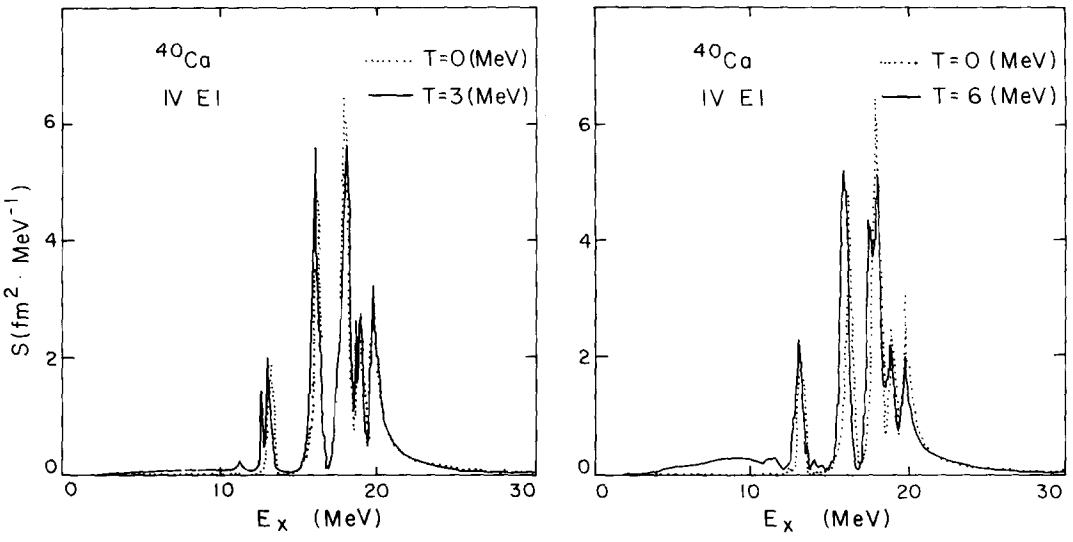

Fig. 2. RPA strength distributions of the IV dipole operator $F(r) = (N/A)\,\Sigma_p r_p Y_{1m}(\hat{r}_p) - (Z/A)\,\Sigma_n r_n Y_{1m}(\hat{r}_n)$ in ^{40}Ca at finite temperatures. The dotted curve shows the result of $T = 0$ MeV, while the solid curves at LHS and RHS correspond to those of $T = 3$ MeV and $T = 6$ MeV, respectively.

trary, the giant resonance has less transition strength at higher temperature and the excitation energy itself is slightly shifted to the higher energy side. This is as we expect: at finite temperature, the giant is less collective and has an energy close to the particle–hole energies of the shells involved. The width Γ of the giant resonance is increasing at higher temperature, i.e., varying from 0.4 MeV at $T = 0$ MeV to 1.2 MeV at $T = 6$ MeV. A more important increase in the width would come from collisional damping which is not calculable within the RPA theory.

The energy moments m_1, m_0, and m_{-1} are tabulated in table 1. The accuracy of the numerical calculation may be checked by comparing with the analytic expression (12), since the Thouless theorem ensures the agreement of two quantities in the self-consistent calculation even at finite temperature [2,5]. The numerical result of the m_1-moment agrees with the analytic value eq. (12) within an error of a few percent in each case. While the EWSR value m_1 is slightly increasing at higher temperature, the values m_0 and m_{-1} are changed very much due to the low-energy excitations induced by finite temperature. Especially, the m_{-1} moment increases rapidly and the value at $T = 3$ MeV reaches more than twice the zero temperature value. This is quite different to the result of the Thomas–Fermi approximation where the shell structure of the strength distribution is not taken into account explicitly [13].

The behavior of the isovector E1 strength function

Table 2
RPA results for IV dipole states (E1) in ^{40}Ca at finite temperatures. The enhancement κ is defined by eq. (13). For details, see the caption to table 1.

T (MeV)	E^* (MeV)	κ	m_1(fm^2 MeV) case (a)	m_1(fm^2 MeV) case (b)	m_0 (fm^2)	m_{-1} (fm^2 MeV^{-1})	$E_1 = (m_1/m_{-1})^{1/2}$	m_0 (E_x<10 MeV)	m_0 (E_x<15 MeV)
0	0	0.330	197.4	195.9	10.68	0.596	18.13	0.0	0.916
3	37.67	0.313	195.0	200.4	11.37	0.691	17.03	0.412	1.41
6	99.54	0.293	192.0	195.5	11.95	0.841	15.25	1.28	2.92

is shown in fig. 2 and table 2. The isovector E1 strength at $T = 0$ MeV in fig. 2 is spread out in a broad energy region $E_x = 13$–20 MeV with the main peak at $E_x = 18$ MeV. The experimental data [14] also show a broad resonance at around $E_x = 20$ MeV. The EWSR value has the temperature dependence only through the enhancement factor κ and decreases at most by a few percent until $T = 6$ MeV. The EWSR m_1(b) estimated from the RPA calculation in table 2 shows a good agreement with the value m_1(a) obtained by the analytic formula (12) at each temperature.

While some transition strength is seen in the low energy region below $E_x = 10$ MeV of fig. 2, i.e., 8% of the total strength at $T = 3$ MeV, the strength distribution of IV dipole states shows much less temperature dependence than the IS strength. The sensitivity of the quadrupole strength function may be understood in part in terms of the softness of the nucleus, which in turn depends on the momentum distribution function of the particles. With a relatively sharp Fermi surface of a closed shell nucleus, a quadrupole deformation requires a corresponding deformation of the momentum distribution, giving a large restoring force [15]. In an open shell nucleus, corresponding to our finite temperature situation, deformation can occur by transitions within a major shell and the strength function has peaks at low excitation. On the other hand, the dipole mode is caused by the displacement of neutrons against protons in coordinate space without any change in momentum space. Thus, the melting of the Fermi surface is not crucial for the excitation energy and the strength distribution of the IV dipole state.

This work is supported by National Science Foundation under grant no. PHY-83-12245.

References

[1] D. Vautherin and N. Vinh Mau, Phys. Lett. 50 (1983) 162.
[2] H.M. Sommermann, Ann. Phys. 151 (1983) 163.
[3] M.E. Faber, J.L. Egido and P. Ring, Phys. Lett. 127B (1983) 5.
[4] O. Civitarese, R.A. Broglia and C.H. Dasso, preprint NBI-83-29 (1983).
[5] D. Vautherin and N. Vinh Mau, preprint IPNO/TH, 83-55 (Orsay, 1983).
[6] J.O. Newton et al., Phys. Rev. Lett. 46 (1981) 1383.
[7] J.E. Draper et al., Phys. Rev. Lett. 49 (1982) 434.
[8] D.H. Dowell et al., Phys. Rev. Lett. 50 (1983) 1191.
[9] G.F. Bertsch and S.F. Tsai, Phys. Rep. 18c (1975) 126.
[10] Nguyen Van Giai and H. Sagawa, Nucl. Phys. A371 (1981) 1.
[11] Nguyen Van Giai and H. Sagawa, Phys. Lett. 106B (1981) 379.
[12] A. van der Woude et al., Contrib. Florence Intern. Conf. on Nuclear Structure (Florence, 1983) p. 241.
[13] J. Meyer, P. Quentin and M. Brack, preprint LYCEN/8350 (1983).
[14] B.L. Berman and F.C. Fultz, Rev. Mod. Phys. 47 (1975) 713.
[15] G.F. Bertsch, Nuclear physics with heavy ion and mesons, ed. R. Balian (North-Holland Amsterdam, 1978) p. 211;
H. Sagawa and G. Holzwarth, Prog. Theor. Phys. 59 (1978) 1213;
G. Holzwarth and G. Eckart, Z. Phys. A284 (1978) 291.